Heteroatomic Stitching of Broken WS_2 Monolayer with Enhanced Surface Potential

Deepa Thakur[1], Yukio Sato[2], Viswanath Balakrishnan[1]*

[1]School of Mechanical and Materials Engineering, Indian Institute of Technology Mandi, Kamand, Himachal Pradesh, India-175075

[2]Department of Materials Science and Engineering, Kyushu University, 744 Motooka, Nishi-ku, Fukuoka, Japan (819-0395)

Email: viswa@iitmandi.ac.in

Supplementary Information:

Figure S1: (a) Illustration of CVD growth of MoS_2 by sulphurising MoO_3 powder. (b) Image of stitched sample grown over SiO_2/Si wafer.

Figure S2: (a) High magnified FESEM images to show (a) crack and (b) stitched crack in WS_2.

Figure S3: (a) active edge length comparison (a) in crack free WS_2 monolayer and (b) cracked WS_2.

Figure S4: STEM-HAADF image of stitched region along with elemental mapping: (a) HAADF image of the selected area is shown. (b) W, (c) Mo and (d) S mapping is shown.

Figure S5: (a) STEM-HAADF image of WS_2-stitch interface as displayed in Fig. 4(b). (b)-(d) Magnified images in the region shown by orange, blue, and green boxes in (a). (e)-(g) Magnified images with overlay of bright contrast showing cation positions. Orange and green open circles denote W and Mo positions, respectively.

Figure S6: (a) AFM height scan and (b) height plot of multilayer MoS_2. (c) KPFM scan and (d) KPFM plot of multilayer MoS_2.

Figure S7: (a) AFM height scan and (b) height plot of multilayer WS_2. (c) KPFM scan and (d) KPFM plot of multilayer WS_2.

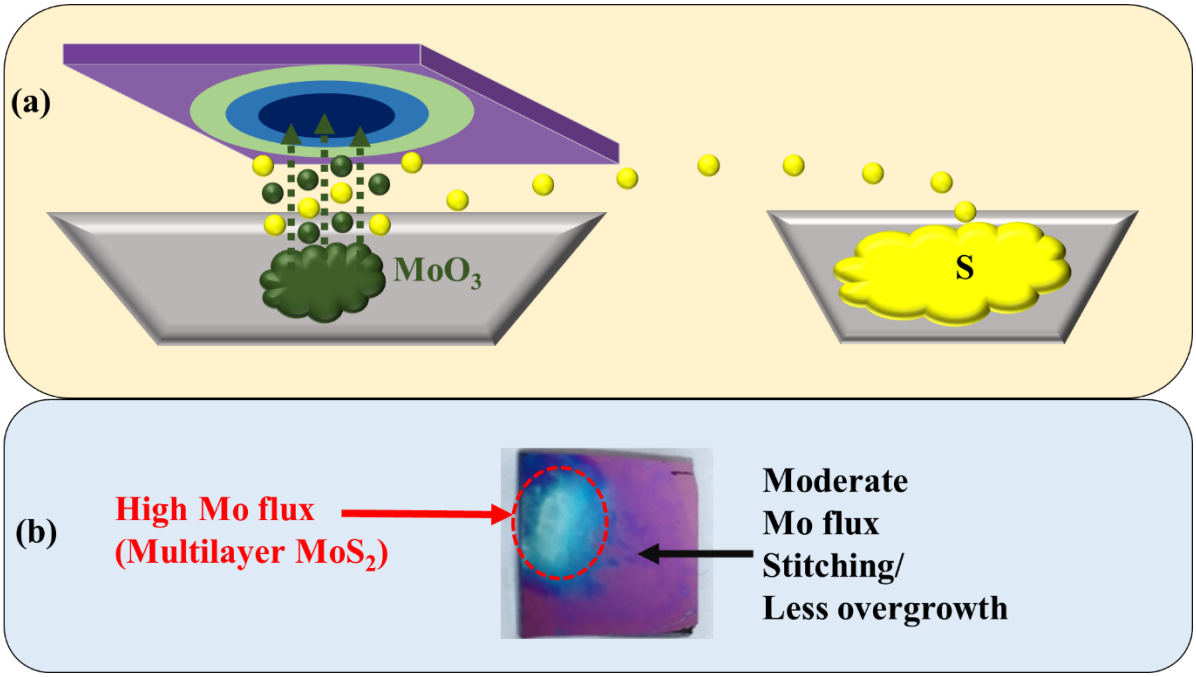

Figure S1: (a) Illustration of CVD growth of MoS_2 by sulphurising MoO_3 powder. (b) Image of stitched sample grown over SiO_2/Si wafer.

CVD growth method was used to grow stitched WS_2. Firstly, cracked WS_2 was grown over SiO_2/Si substrate followed by MoS_2 growth. Here MoS_2 growth was achieved by sulphurising MoO_3 in Ar environment (figure S1a). Here MoO_3 was taken in powder form. During formation of MoS_2, those areas on the substrate which were near MoO_3 powder get more precursor flux. Closer areas were observed to grow bulk like and Multilayer MoS_2. Here vertical growth of MoS_2-WS_2 heterostructure was observed to dominate. On moving away from high flux region to moderate flux region, MoS_2 layer number was observed to decrease and stitched regions were found. In figure S1b, image of a sample wafer is shown. The area marked with red circle have high precursor flux and due to which multilayer MoS_2 growth dominate this region. The areas outside this red circle have moderate flux and corresponds to the region where stitched WS_2 were grown.

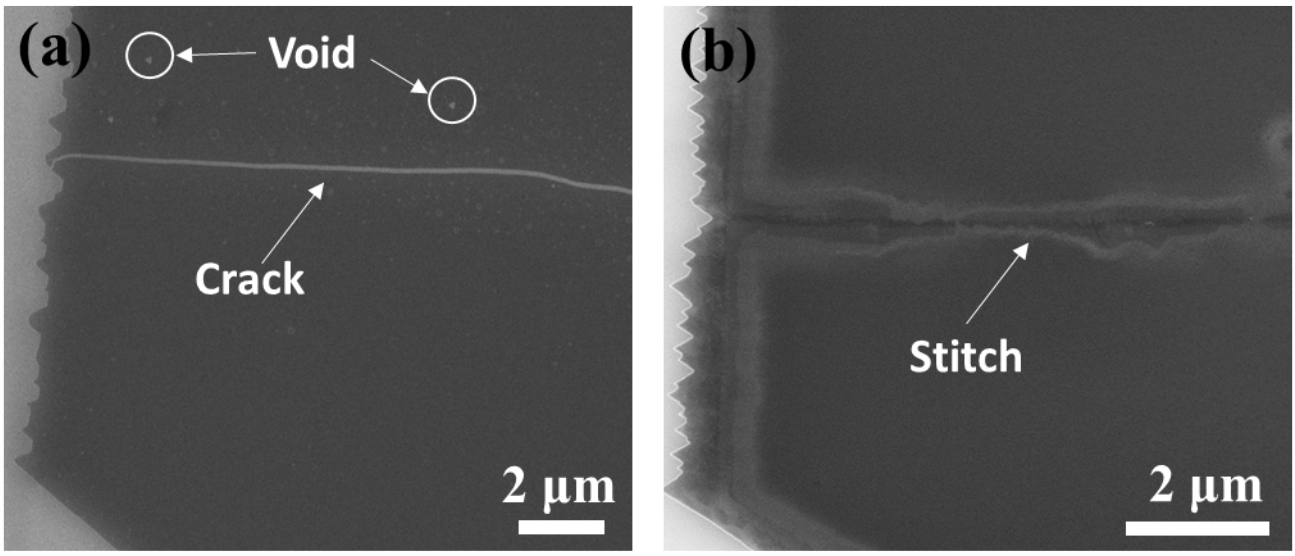

Figure S2: (a) High magnified FESEM images to show (a) crack and (b) stitched crack in WS_2.

The first figure S2a shows the WS_2 prior to the growth of MoS_2. Initially WS_2 is cracked and have small voids as well. Voids are marked inside white circles. The crack is grey colored line discontinuing the WS_2 into two fragments. This crack is filled after the growth of MoS_2. The growth of MoS_2 is also observed in the outer edges of WS_2 flake as well. After the MoS_2 growth, both the fragmented parts of WS_2 are joined as shown in S2b.

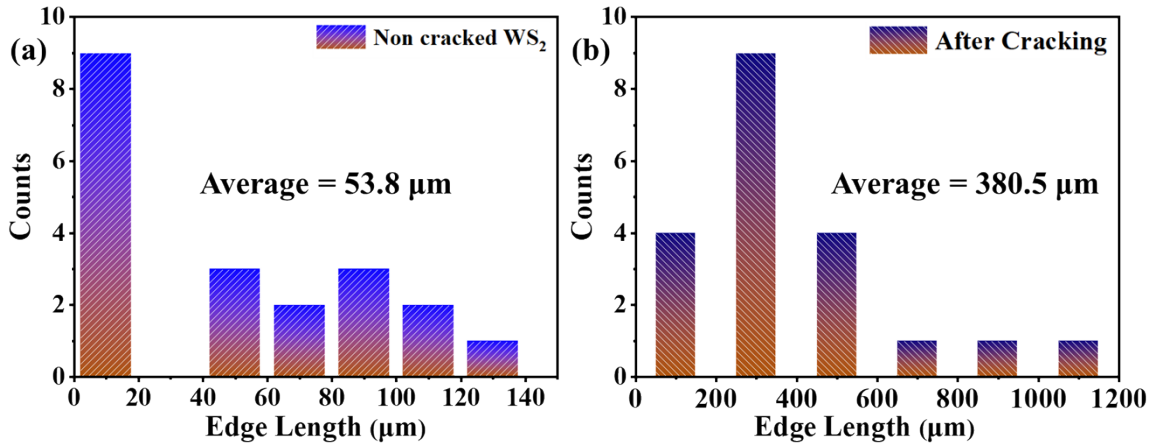

Figure S3: (a) active edge length comparison (a) in crack free WS_2 monolayer and (b) cracked WS_2.

Edges have unsatisfied dangling bonds which act as active site for many applications like catalysis, electrochemistry, adsorption etc. It was observed that smaller domains are free from cracks and voids. The average edge length in crack free WS_2 was 53.8 µm as calculated in

figure S3a. Whereas active edge length was observed to increase in after formation of cracks in WS_2. The average edge length in fractured WS_2 was calculated to be 380.5 μm as shown in figure S3b. Cracking in WS_2 have ability to increase the active edges by ~7X, as evaluated from edge length histograms.

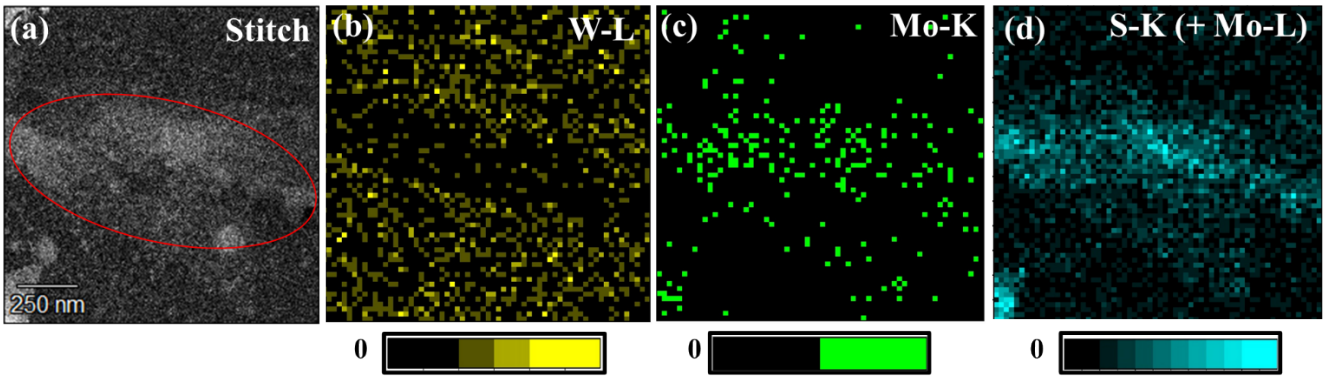

Figure S4: STEM-HAADF image of stitched region along with elemental mapping: (a) HAADF image of the selected area is shown. (b) W-L, (c) Mo-K and (d) S-K (+ Mo-L) mapping is shown.

The red oval region shown in S4a is the MoS_2-Stitch. In the W-L mapping shown in figure S4b, middle region is W deficient and on the other sides W is present. Figure S4c shows the Mo-K map. The Mo signal is present only in the middle region near to W deficient area. Figure S4d presents the S-K (+ Mo-L) map. Because X-ray energy for the S-K line (~ 2.307 keV) was close to that for the Mo-L line (~ 2.293 keV), the S-K map should also include the Mo-L signal. The signal of S is present everywhere which is due to presence of S in WS_2 as well as in MoS_2. More intense signal in the middle can be due to the presence of multilayer MoS_2 as well as detection of the Mo-L signal.

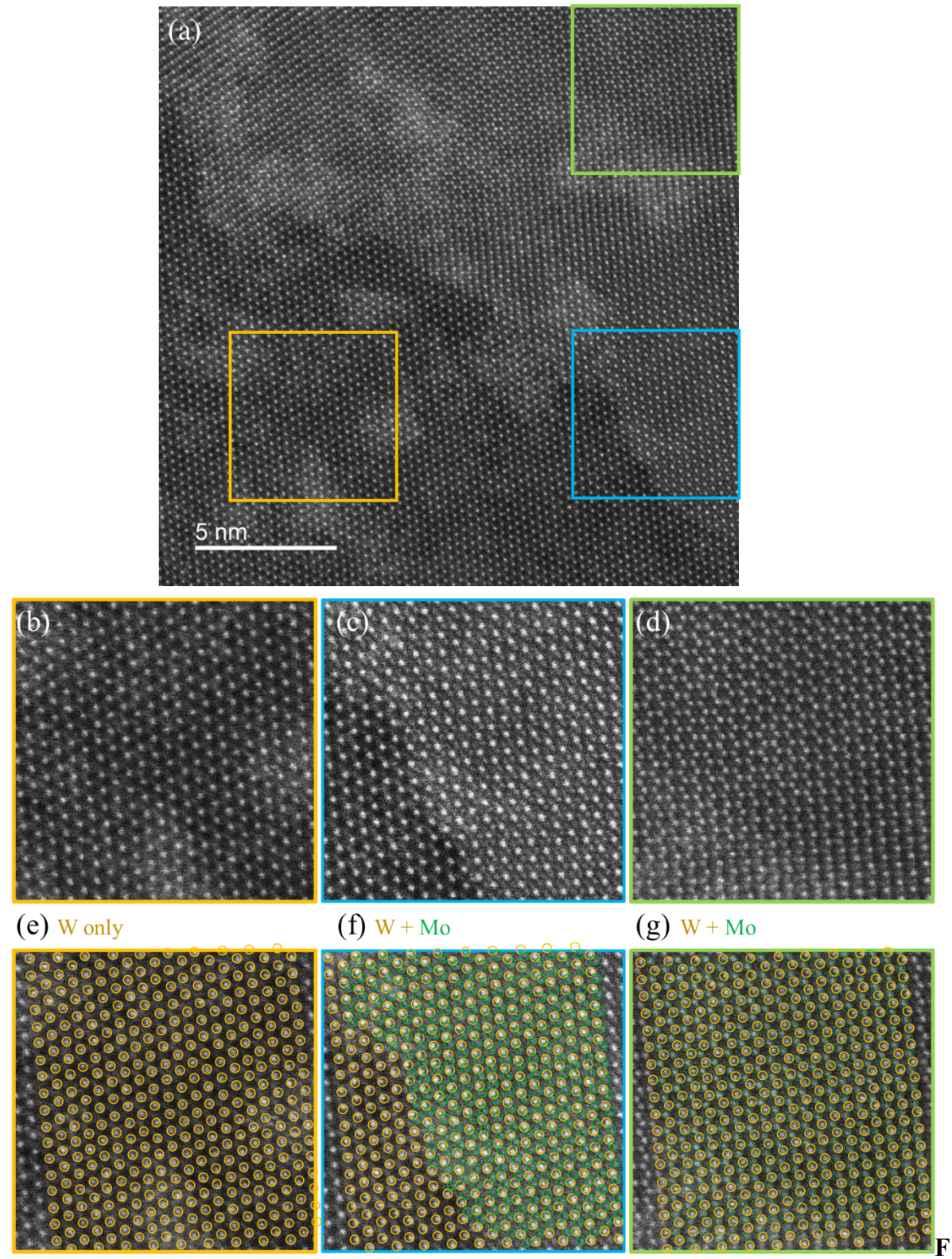

Figure S5: (a) STEM-HAADF image of WS_2-stitch interface as displayed in Fig. 4(b). (b)-(d) Magnified images in the region shown by orange, blue, and green boxes in (a). (e)-(g) Magnified images with overlay of bright contrast showing cation positions. Orange and green open circles denote W and Mo positions, respectively.

Figure S5(a) shows the interface between the WS_2 and stitch. Note that bright contrast indicates position of heavy element such as W and Mo, because contrast of STEM-HAADF image is

dependent on atomic number of constituting ions. In the left-bottom region (Fig. S5(b)), only WS_2 layer was observed, in which W positions were observed as hexagonal lattice. In the right-bottom side (Fig. S5(c)), additional contrast due to presence of Mo overlapped in addition to the contrast for W, which was due to the overgrowth of MoS_2. Furthermore, the overlapping pattern looked different in the top-right region (Fig. S5(d)). This was due to the lattice mismatch between the WS_2 and MoS_2 layers. The difference was quite small, shift of the MoS_2 lattice occurred a little by a little. Therefore, the shift could not be recognized without investigating a wide region. These points were highlighted in Fig. S5(e)-(g) by overlaying W and Mo positions by open circles. From the comparison between Fig. S5(f) and (g), it was clarified that MoS_2 lattice was slightly shifted due to small lattice mismatch between the WS_2 and MoS_2 layers.

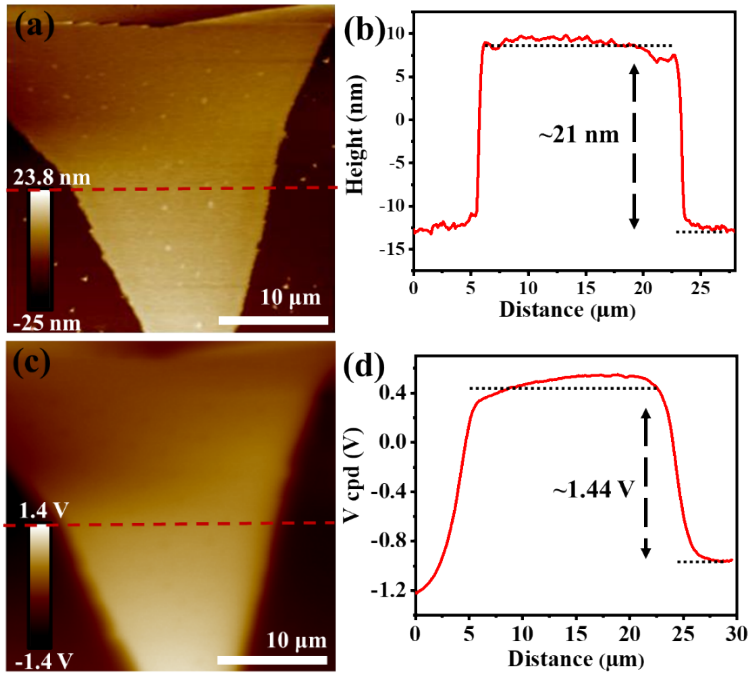

Figure S6: (a) AFM height scan and (b) height plot of multilayer MoS_2. (c) KPFM scan and (d) KPFM plot of multilayer MoS_2.

In the present work, multilayer MoS_2 stitches the fractured WS_2. In order to illustrate the work function of pristine MoS_2 before the heterostructure formation, AFM and KPFM measurement were done. AFM height scan is shown in figure S6a. The line scan taken from this flake is plotted in S6b. The height difference from substrate indicates towards the ~21 nm thickness. The KPFM image of same flake is presented in figure S6c. The quantitative analysis shown in figure S6d indicates ~1.44V potential difference between MoS_2 and substrate.

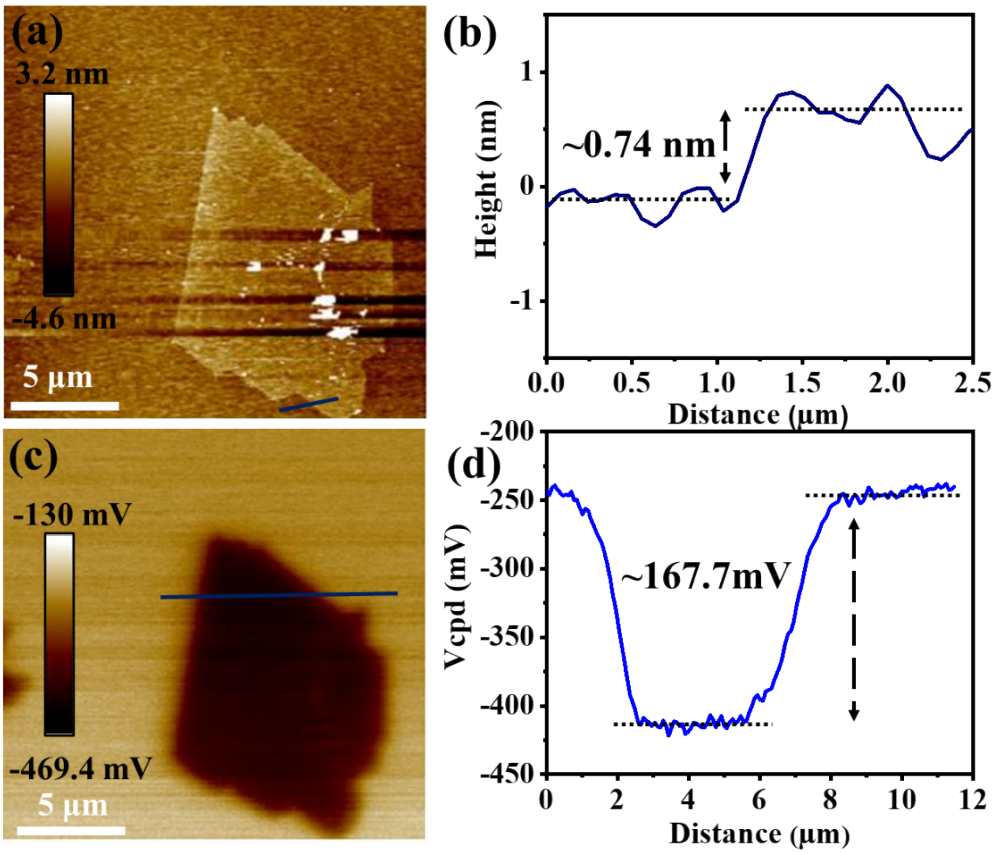

Figure S7: (a) AFM Height scan and (b) height plot of multilayer WS_2. (c) KPFM scan and (d) KPFM plot of multilayer WS_2.

In order to probe the work function of pristine WS_2 before the heterostructure formation, AFM and KPFM measurements were performed. AFM height scan is shown in figure S7a. The height line profile taken from this flake is plotted in S7b. The height difference from substrate is found to be around ~ 0.74 nm in thickness. This indicates single layer nature of WS_2. The KPFM image of same flake is presented in figure S7c. The quantitative analysis shown in figure S6d indicates ~167.7mV potential difference between substrate and MoS_2.

The calculated difference in fermi levels between individual MoS_2 and WS_2 is shown below.

From the literature[1,2] it is known that

$$e.V_{cpd} = \phi_{tip} - \phi_{material} \quad \text{.....(S1)}$$

Where Vcpd represents contact potential difference and ϕ represents work function. Now using same equation for Substrate SiO_2/Si, MoS_2 and WS_2 we get,

$e.V_{cpd\,WS2} = \phi_{tip} - \phi_{WS2}$……..……(S2)

$e.V_{cpd\,MoS2} = \phi_{tip} - \phi_{MoS2}$……...……..(S3)

$e.\ V_{cpd\,SiO2} = \phi_{tip} - \phi_{SiO2}$……...…….(S4)

As the measurements of WS_2 and MoS_2 are performed on SiO_2/Si substrate individual material needs to be corrected with respect to substrate. Subtracting equation (S2) from equation (S4) and equation (S3) from equation (S4) we get

$e.\Delta V_{cpd1} = V_{cpd\,SiO2} - V_{cpd\,WS2} = \phi_{WS2} - \phi_{SiO2}$ ……..……..(S5)

$e.\Delta V_{cpd2} = V_{cpd\,SiO2} - V_{cpd\,MoS2} = \phi_{MoS2} - \phi_{SiO2}$ ……..……(S6)

Now, subtracting equation (S6) from equation (S5), we get

$e.\Delta V_{cpd1} - e.\Delta V_{cpd2} = V_{cpd\,MoS2} - V_{cpd\,WS2} = \phi_{WS2} - \phi_{MoS2}$……(S7)

Taking values from figure S4 and S5, we have

$\Delta V_{cpd1} = V_{cpd\,SiO2} - V_{cpd\,WS2} = 0.1677\ V$

$\Delta V_{cpd2} = V_{cpd\,SiO2} - V_{cpd\,MoS2} = -1.44\ V$

Using these values in eqn 7 we get:

$e.[0.1677\ V - (-1.44\ V)] = \phi_{WS2} - \phi_{MoS2}$

Or $e.(1.6077\ V) = \phi_{WS2} - \phi_{MoS2}$

Or $\Delta EF = \phi_{WS2} - \phi_{MoS2} = 1.6\ eV$

This calculation suggests that work function of single layer WS_2 is more than multilayer-MoS_2. This supports the validity of band structure shown in figure 8c. The values of ΔE_F can vary based on layer numbers of MoS_2 as well as WS_2.

References:

(1) Choi, S. H.; Shaolin, Z.; Yang, W. Layer-Number-Dependent Work Function of MoS_2 Nanoflakes. *J. Korean Phys. Soc.* **2014**, *64* (10), 1550–1555. https://doi.org/10.3938/jkps.64.1550.

(2) Strategy, T. L. E.; Chen, K.; Wan, X.; Wen, J.; Xie, W.; Kang, Z.; Zeng, X.; Al, C. E. T. Electronic Properties of MoS_2-WS_2 Heterostructures Synthesized with Two-Step Lateral Epitaxial Strategy. *ACS Nano* **2015**, *9* (10), 9868–9876. https://doi.org/10.1021/acsnano.5b03188.